Applied Surface Science 442 (2018) 517–524

Contents lists available at ScienceDirect

Applied Surface Science

journal homepage: www.elsevier.com/locate/apsusc

Full Length Article

Properties, ageing behavior and stability of bipolar films containing nano-layers of allylamine and acrylic acid plasma polymers

Gaelle Aziz [a,*], Mahtab Asadian [a], Heidi Declercq [b], Rino Morent [a], Nathalie De Geyter [a]

[a] Research Unit Plasma Technology (RUPT), Department of Applied Physics, Faculty of Engineering & Architecture, Ghent University, Belgium
[b] Tissue Engineering and Biomaterials Group, Department of Basic Medical Sciences, Ghent University, Belgium

ARTICLE INFO

Article history:
Received 3 August 2017
Revised 12 February 2018
Accepted 19 February 2018
Available online 21 February 2018

Keywords:
Plasma polymerization
Bipolar film
Allylamine
Acrylic acid
Surface analysis

ABSTRACT

In this work, a dielectric barrier discharge (DBD) has been used for the deposition of bipolar films containing alternating nano-layers of plasma polymerized allylamine (PPAam) and acrylic acid (PPAac). Various films were obtained by varying the single-layer thickness of each plasma polymer while maintaining a constant total film thickness and two kinds of films were fabricated via different depositing sequences (PPAam/Aac and PPAac/Aam). Films properties, ageing in air and stability in water over a 7 days period were investigated. Results showed that, COO^- and NH_3^+ polar entities, generated from the interaction of PPAam and PPAac, are present in the bipolar films. Concerning the films stability, the different reaction mechanisms involved in the formation of each kind of films resulted in a higher amount of polar groups in the PPAam/Aac films; this conferred these films a higher stability than PPAac/Aam. Concerning the films ageing behavior, all prepared samples underwent some kind of ageing which was found to be dependent on the deposition sequence. Results also showed that bipolar coatings exhibited better cell-material interactions compared to PPAam and PPAac films; with a better cell viability observed on PPAam/Aac coatings after 1 and 7 days culture.

1. Introduction

Chemical inertness is the main weakness of polymer materials when placed in contact with biological environments. Known for their good chemical reactivity, primary amines (—NH_2) and carboxyl (—COOH) can be used to tailor a polymer surface in order to overcome this issue. Moreover, in aqueous solution at physiological pH value, the protonated/deprotonated amino/carboxyl groups can introduce localized positive/negative charges to the surface thus increasing its affinity for cells, proteins and biomolecules [1–3]. This can provide different "anchor" sites usable for grafting biomolecules with different activities on the same substrate.

Total joint replacement (TJR) is a procedure in which damaged joints are replaced with an artificial device. Though TJR are mostly successful, in time, the artificial joints can become loose and unstable due to wear, requiring expensive and undesirable revision surgery. Implant durability and reliability are mostly determined by the properties of the articulating surfaces in TJRs. For example, in a hip joint, the interface between the femoral head and acetabular cup lining is critical in determining the implant lifespan. Previously, stainless steel heads and Teflon liners were used [4]. Nowadays, the evolution of material pairs used for this interface has led to the extensive use of the combination of an ultra-high molecular weight polyethylene (UHMWPE) liner and metallic or ceramic femoral heads [5–7]. However, in arthroplasty, a major unsolved problem is the mechanical wear of the artificial joint which limits the lifetime of the implant [8]. The average lifetime of artificial hip joints incorporating UHMWPE is only 15–20 years.

In the natural joint, lubrication is provided by the synovial fluid. Following arthroplasty, a fluid of similar composition surrounds the artificial joint. Synovial fluid contains, among others, a substantial amount of albumin protein. Protein adsorption is highly affected by protein conformation and polymer surface hydrophilicity which in turn affects the resulting friction in the joint. Unfolded proteins preferentially adsorb onto hydrophobic polymer surfaces and increase sliding friction. This can be largely suppressed by rendering the substrate more hydrophilic. More hydrophilic surfaces preferentially adsorb proteins of native conformation, which form thicker, denser films that have the potential to reduce boundary-lubricated friction [9].

Widmer et al. [10] showed that hydrophobic polyethylene surfaces exhibit higher friction than hydrophilic ones. By using optical waveguide lightmode spectroscopy, they showed that proteins adsorbed onto hydrophobic surfaces occupy more surface area

* Corresponding author.
E-mail address: gaelle.aziz@ugent.be (G. Aziz).

https://doi.org/10.1016/j.apsusc.2018.02.190
0169-4332/

than those adsorbed onto hydrophilic surfaces. They therefore suggested that proteins denature during adsorption onto hydrophobic surfaces. This protein behavior has also been reported in relation to other applications [11,12].

Natural cartilage is composed of cells named chondrocytes and the extracellular matrix (ECM) produced by these cells. The ECM molecules in cartilage include proteoglycans, hyaluronan or hyaluronic acid (HA), type II collagen, glycoproteins and various elastic fibers.

Our approach is to render the UHMWPE surface more hydrophilic and thus make it more similar to that of natural cartilage where the surface consists of very hydrophilic species, i.e. proteoglycans. Aggrecan is the major proteoglycan in the articular cartilage and the most crucial to its proper functioning. Aggrecan is a multifaceted molecule expressed by chondrocytes and having an amino and a carboxyl terminus [10].

In this study, positively/negatively charged surfaces based on plasma polymerized multistacked allylamine (Aam) and acrylic acid (Aac) films which contain alternating nano-layers of the —NH_2 and —COOH functional groups were prepared. Different sets of monomer single-layer with a total thickness of 180 ± 20 nm were synthesized and two kinds of coatings were obtained by changing the deposition sequence of Aam and Aac single-layers.

The chemical and physical properties of these films were investigated using XPS and WCA analysis. Ageing behavior at ambient atmosphere for a period of 7 days was investigated using XPS and WCA analysis. Coatings stability after soaking in D.I. water for 7 days was also evaluated using XPS and OPS analysis. Moreover, cell tests using human foreskin fibroblasts were performed and evaluations were conducted after 1 and 7 days of culturing.

2. Materials and methods

2.1. Materials

Allylamine (98%) was purchased from Sigma-Aldrich. Helium (Alphagaz 1) used for plasma activation and helium used as carrier gas during plasma polymerization was purchased from Air Liquide and was used as supplied. UHMWPE (0.075 mm thick) and PET (0.1 mm thick) films were ordered from Goodfellow (Cambridge, UK) and were not subjected to any pretreatment step prior to plasma modification. Rectangular samples of $2 * 1\ cm^2$ were cut for treatment and subsequent physic-chemical studies.

2.2. Plasma treatments

Plasma treatments were performed using 2 similar DBD set-ups, one for each monomer; transfer time between both reactors was less than a minute. A schematic diagram of the used DBD set-ups is depicted in Fig. 1.

Both reactors were identical except for the following: - the first experimental set-up which was used for allylamine consists of two circular copper electrodes (diameter = 40 mm) covered with a ceramic dielectric and separated by a distance of 6 mm and a gas inlet parallel to the inter-electrode space; all of which are placed in a cylindrical enclosure. The upper electrode is connected to a high frequency (58 kHz) AC power source, and the lower electrode to earth through a resistor R (50 Ω) or a capacitor C (10 nF); - the second experimental set-up which was used for acrylic acid consists of two copper electrodes. The lower electrode is embedded in a ceramic crucible and connected to a high frequency (50 kHz) AC power source. The upper electrode is porous covered with a ceramic coating and connected to earth through a resistor R (100 Ω) or a capacitor C (10.4 nF) (electrode configuration can be seen in [13]). Space between the two electrodes is 7.7 mm and

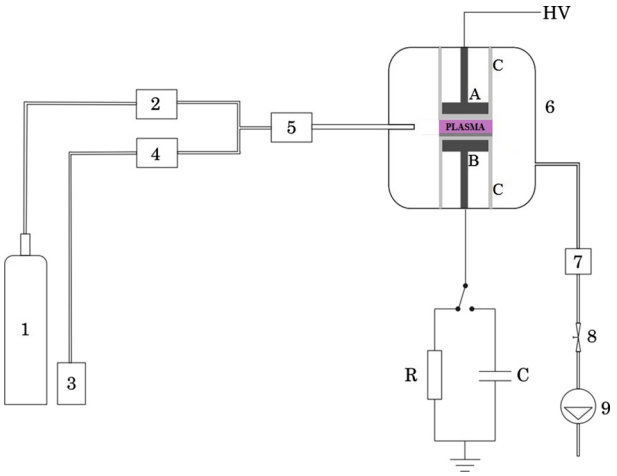

Fig. 1. Schematic representation of the used DBD set-ups (1-Helium container, 2-Mass flow controller for helium, 3- Allylamine/acrylic acid container, 4- Mass flow controller for allylamine/acrylic acid, 5-CEM® system, 6- Plasma reactor "A- HV electrode, B- Ground electrode, C- dielectrics", 7- Pressure gauge, 8- Valve, 9-Pump).

the gas inlet is connected to the reactor on the topside where the upper electrode is located. The gap between the gas inlet and upper electrode is filled with a glass wool filler that helps to distribute the gas flow more evenly before entering the plasma discharge region.

During the experiments, the substrate (UHMWPE/PET) is fixed with tape on the lower dielectric. First, the discharge chamber is pumped down to 0.01–0.03 kPa using a rotary vane pump then it is filled with helium using a Bronkhorst El-Flow® mass flow controller at a rate of 3 slm (standard liter per minute). The pressure in the chamber is then maintained at 90 kPa for 3 min by a needle valve: this is a purging step. The pumping and purging steps are done to control the chamber environment. Afterwards, the helium flow rate is lowered to 1 slm, the pressure to 5 kPa and the films are plasma-treated for 60 s at 1.2 W in order to ensure that the substrate surfaces are saturated with functional groups. This pre-polymerization step is performed to increase the subsequent deposited coating adhesion to the substrate.

For the polymerization step, the system is brought to the desired pressure with the predefined helium and monomer flow rates. In each reactor, Aam and Aac are dosed using a Bronkhorst mini CORI-FLOW® meter (type M12) and are mixed with He in a Bronkhorst controlled evaporation module (CEM®, type W-202A) before the mixture is sent via the gas inlet into the reactor between the two electrodes. Plasma is then turned ON with a predetermined discharge power and for a specific period of time. Plasma treatments were performed at atmospheric (100 kPa) and sub-atmospheric (50 kPa) pressures for both Aam and Aac plasma polymers, respectively.

In previous works [13,14], we investigated the plasma parameters effects on the properties and stability of allylamine and acrylic acid plasma polymer coatings deposited onto UHMWPE substrates. Results showed that the 24.0 W–1 g/h and 27.0 W–0.25 g/h treatment conditions resulted in the most stable coatings while maintaining a high amino/carboxyl concentrations, for allylamine and acrylic acid studies, respectively.

In this study, bipolar films were prepared using these parameters while varying the Aam and Aac deposition times and deposition sequence as summarized in Table 1. In this Table, the 1st layer refers to the plasma polymer coating directly deposited on the UHMWPE substrate surface while the 2nd layer refers to the plasma polymer coating deposited on top of the 1st layer.

Table 1
Summary of the used treatment times for both sets of bipolar films.

Bilayer sample with layer thickness	Deposition time (s)	
	1st layer PPAam	2nd layer PPAac
PPAam-100 nm/Aac-80 nm	50	20
PPAam-120 nm/Aac-60 nm	55	15
PPAam-140 nm/Aac-40 nm	60	10
	1st layer PPAac	2nd layer PPAam
PPAac-100 nm/Aam-80 nm	60	40
PPAac-120 nm/Aam-60 nm	90	20
PPAac-140 nm/Aam-40 nm	120	10

2.3. Ageing test

The ageing behavior of the various prepared bipolar coatings was studied after storing the samples for a period of 7 days in a BINDER KMF 115 climate chamber which provides a stable environment for sample storage. In this study, temperature (T) and relative humidity (RH) were fixed (T = 20 °C, RH = 30%) with fluctuations of less than 0.2 °C and 2.5% respectively.

2.4. Stability test

For the stability behavior of the various prepared bipolar coatings, samples were soaked in deionized water (D.I.) and stored in a thermo-controlled bath (Julabo SW22) at 37 °C for 7 days. Deionized water was chosen as test medium because it does not contain any compounds that might deposit on the sample surface and interfere with subsequent surface analyses. Afterwards, samples were stored overnight under vacuum to evaporate the water that can be trapped in the coating.

2.5. Surface characterization

2.5.1. X-ray photoelectron spectroscopy (XPS)

The chemical composition of the UHMWPE samples is investigated by X-ray photoelectron spectroscopy (XPS), which is performed on a PHI 5000 Versaprobe II spectrometer employing a monochromatic Al K_α X-ray source ($h\nu$ = 1486.6 eV) operating at 23.3 W. The pressure in the analyzing chamber is maintained at 10^{-9} kPa or lower during analysis and the photoelectrons were detected with a hemispherical analyzer positioned at an angle of 45° with respect to the normal of the sample surface. Survey scans and individual high resolution spectra N1s/C1s were recorded with a pass energy of 187.85 eV (eV step = 0.8 eV) and 23.5 eV (eV step = 0.1 eV), respectively. On each sample surface 3 spots (500 * 500 μm) were selected for measurement. The elements present on the UHMWPE surfaces were identified and quantified from the XPS survey scans using Multipak software (Version 9.6.1). The relative sensitivity factors of the elements were provided by the manufacturer (C = 0.314; O = 7.33; N = 0.499).

Using the same Multipak software, XPS curve-fitting was also performed in order to characterize the chemical environment of the elements and thus identify and quantify the various contributions of the different formed chemical species. The hydrocarbon component of the C1s spectrum (285.0 eV) was used to calibrate the energy scale and the peaks were deconvoluted using Gaussian-Lorentzian peak shapes and a Shirley background. Curve fittings were all performed with a full width at half maximum (FWHM) between 1.2 and 1.6 and a chi-square value less than 1 indicating a good fit. Surface atomic composition and atomic bonds percentages are the average of the ones obtained for the 3 selected spots on the surface.

2.5.2. Water contact angle (WCA)

WCA measurements were carried out with a commercial Krüss Easy Drop optical system (Krüss GmbH, Germany). Measurements were taken on a 1 μl D.I. water drop at ambient temperature using Laplace-Young curve fitting. For each condition, three samples were made and for each of them six WCA values were measured at various locations of the analyzed surface. Reported contact angles are the average of these measurements. Standard deviations were less than or equal to 3°.

2.5.3. Optical reflectance spectroscopy (OPS)

In order to measure the thickness of the deposits and subsequently evaluate their stability, OPS measurements were conducted on PET films using a Filmetrics F20 device. PET was chosen over UHMWPE as a substrate because of its good reflective properties and its low natural roughness (≈10 nm). Individual films thicknesses were measured for each monomer before layering both allylamine and acrylic acid films thus forming the bipolar layers whose thicknesses were also measured for better precision. OPS can determine the thickness of the coating by first measuring the spectral reflectance of the coating using the interference pattern between the reflected light beam from the coating surface and the substrate and subsequently fitting the resulting spectra. For each condition, to investigate the thickness of the deposited layers, 2 samples were made and 10 spots per sample were measured. Thickness values were the average of all measured spots.

2.6. Cell culture and cell/biomaterial tests

2.6.1. Cell culture and cell seeding onto the UHMWPE films

HFF-1 cells (human foreskin fibroblasts, ATCC) were cultured in DMEM glutamax medium (Gibco Invitrogen) supplemented with 10% foetal bovine serum (FBS, Gibco Invitrogen), 2 mM L-glutamine (Sigma-Aldrich, Belgium), P/S (10 U/ml penicillin, 10 mg/ml streptomycin, Gibco Invitrogen) and 100 mM sodium pyruvate (Gibco Invitrogen). Cells were cultured at 37 °C in a humidified atmosphere containing 5% CO_2. UHMWPE films (diameter 14 mm) were left untreated or subjected to plasma treatment. Sterilization was performed by ethanol rinsing before plasma treatment and subjecting to UV light (30 min) after plasma treatment.

For the cell proliferation assay, cells were seeded at a density of 40,000 cells/ml medium per film in 24-well culture dishes and evaluated after 1 and 7 days.

2.6.2. MTS viability

The colorimetric MTS assay (CellTiter 96® Aqueous non-radioactive cell proliferation assay, Promega), using a tetrazolium compound [3-(4, 5-dimethylthiazol-2-yl)-5-(3-carboxymethoxy phenyl)-2H-tetrazolium, inner salt; MTS] and an electron coupling reagent (phenazine methosulfate; PMS) was performed to quantify cell viability and proliferation on the UHMWPE films. MTS is bioreduced by cells into a formazan product that is soluble in tissue culture medium.

The cell culture medium on the UHMWPE films was replaced by 0.5 ml culture medium (phenol red free DMEM containing 10% FBS) supplemented with 0.1 ml MTS/PMS solution and incubated at 37 °C. After 4 hours, 0.5 ml was transferred to a 24-well tissue culture plate and the absorbance was measured at 490 nm (Universal microplate reader EL 800, Biotek Instruments). Triplicate measurements were performed at the same time points as the microscopic evaluation. Percentage viability was calculated relative to control cultures.

3. Results and discussions

This study aims towards sequentially deposited high functional density film networks of allylamine and acrylic acid plasma layers having a strong interface. It consists of 3 parts: in the first part, the chemical and physical properties of the prepared bipolar coatings are investigated in order to see the influence of the used treatment conditions on the resulting films. In the second and third part, ageing and stability studies are conducted in order to evaluate these behaviors in the different prepared coatings and correlate them to the used experimental conditions.

3.1. Chemical and physical structure of plasma polymeric films

Bipolar films properties were investigated using XPS and WCA analysis. XPS is performed to reveal the top 10 nm surface chemistry of the films while WCA is performed to characterize the outermost surface layer chemistry.

3.1.1. XPS analysis

Based on XPS survey scans, the surface atomic composition of the films can be determined and the results are shown in Table 2. For the PPAam/Aac samples where the first layer is an Aam plasma polymer and the second layer an Aac plasma polymer, it was observed that the percentage of nitrogen detected in the top 10 nm layer is no more than 6.0% and this percentage decreases with Aac treatment time to reach 3.1% for an Aac plasma deposition of 80 nm. The oxygen percentage however, is much higher (29.5% for an Aac plasma deposition of 40 nm) and increases with Aac deposition time to around 32.0% for an Aac plasma deposition of 80 nm. For the PPAac/Aam samples where the first layer is an Aac plasma polymer and the second layer an Aam plasma polymer, it was observed that the percentage of O incorporated for a 40 nm Aam deposit is 20.1%; moreover, this O% decreases with an increase in Aam deposition time. The N% for an 80 nm Aam deposit is around 13.5% and this% decreases with a decrease in Aam deposition time.

As can be seen for all samples, both N and O are present in the surface top 10 nm layer which can be associated to rearrangements in the first plasma polymer during the second layer deposition. This is due to the fact that, during plasma deposition, there are two competing processes that occur. One is the deposition of the film and the other is the ablation of both the already deposited film and the film being deposited. As described above and as seen in Table 2, the thinner the second layer (shorter deposition times) the more pronounced the rearrangement effect on the surface chemical composition. Moreover, one should note that oxygen can also be incorporated to the surface via the reaction of radicals with the atmosphere which explains the high O percentage incorporated at the surface of PPAac/Aam films.

Surface atomic composition of pure PPAac and PPAam coatings were added as reference. As can be seen, the amount of O and N incorporated after sufficient depositions of both Aac (80 nm) and Aam (60 nm) in PPAam/Aac and PPAac/Aam coatings respectively is very similar to that incorporated in the respective pure PPAac and PPAam coatings.

Table 2
Surface atomic composition of PPAac, PPAam, PPAam/Aac and PPAac/Aam coatings.

Sample	C (%)	N (%)	O (%)
PPAac	67.0 ± 0.4	0.0 ± 0.0	33.0 ± 0.6
PPAam	80.4 ± 0.2	13.9 ± 0.6	5.6 ± 0.4
PPAam-100 nm/Aac-80 nm	64.9 ± 1.2	3.1 ± 0.6	32.0 ± 0.8
PPAam-120 nm/Aac-60 nm	66.5 ± 0.7	4.3 ± 0.9	29.2 ± 1.5
PPAam-140 nm/Aac-40 nm	64.5 ± 0.6	6.0 ± 0.5	29.5 ± 1.1
PPAac-100 nm/Aam-80 nm	74.8 ± 1.0	13.5 ± 0.2	11.7 ± 1.0
PPAac-120 nm/Aam-60 nm	72.8 ± 1.3	13.0 ± 0.3	14.2 ± 1.1
PPAac-140 nm/Aam-40 nm	69.9 ± 1.1	9.9 ± 0.5	20.1 ± 1.6

Figs. 2 and 3 show the high-resolution C1s and N1s spectra with the extracted chemical group concentrations of plasma polymerized Aam and Aac films as well as the bipolar films formed by the layering of both films. As can be seen in Fig. 2a, C1s peak deconvolution of an Aam plasma polymer film shows 3 peaks: a peak at 285.0 ± 0.1 eV which corresponds to C—C/C—H bonds, a peak at 2 86.4 ± 0.1 eV which corresponds to C-$NH_{1,2}$ bonds, and a peak at 287.5 ± 0.2 eV which corresponds to CONH bonds [15]. As can be seen in Fig. 2b, C1s peak deconvolution of an Aac plasma polymer film shows 4 peaks: a peak at 285.0 ± 0.1 eV which corresponds to

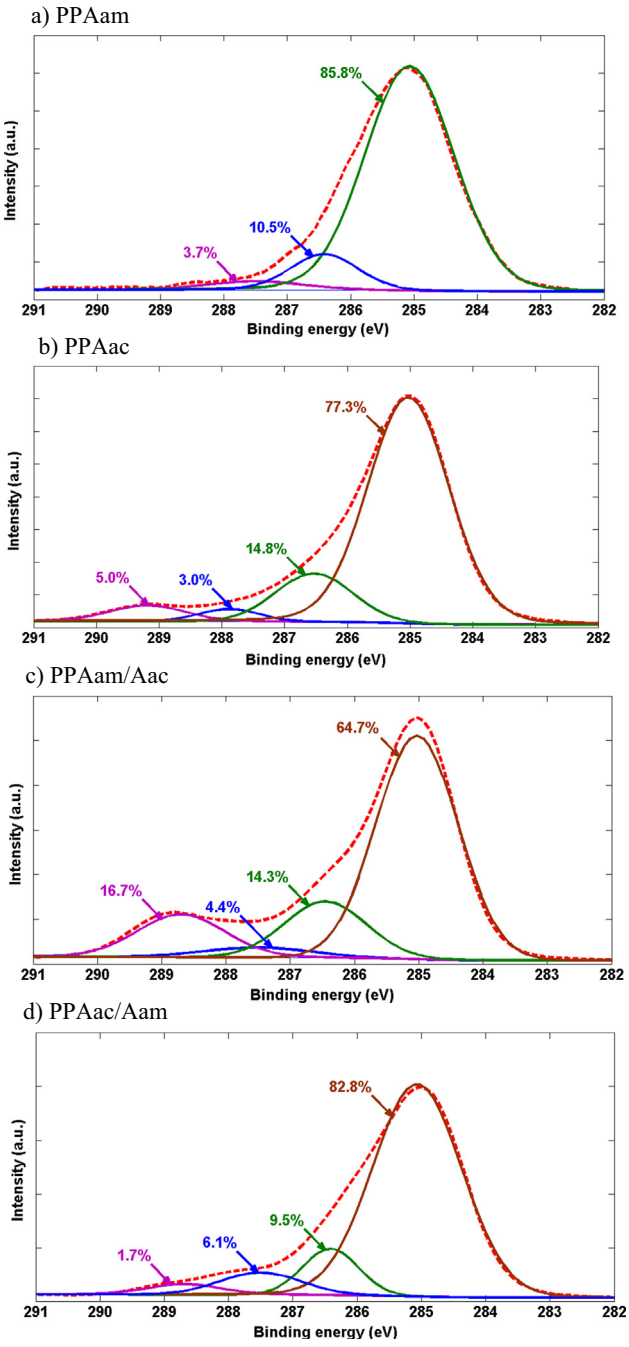

Fig. 2. High resolution C1s XPS peaks of (a) plasma polymerized allylamine (PPAam), (b) acrylic acid (PPAac), and the bipolar film obtained by the sequential deposition of (c) allylamine followed by acrylic acid (PPAam/Aac) and (d) acrylic acid followed by allylamine (PPAac/Aam).

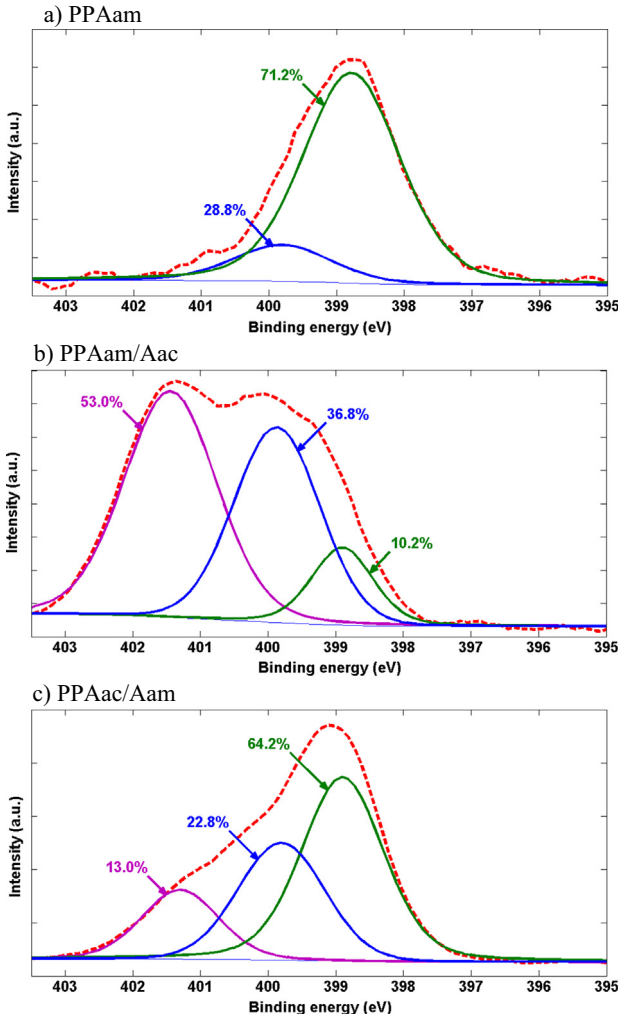

Fig. 3. High resolution N1s XPS peaks of (a) plasma polymerized allylamine (PPAam), and the bipolar film obtained by the sequential deposition of (b) allylamine followed by acrylic acid (PPAam/Aac) and (c) acrylic acid followed by allylamine (PPAac/Aam).

C—C/C—H bonds, a peak at 286.5 ± 0.1 eV which corresponds to C—O—C, C—OH bonds, a peak at 287.7 ± 0.2 eV which corresponds to C=O bonds, and a peak at 289.2 ± 0.1 eV which corresponds to COOH, COOR bonds [16]. As can be seen in Fig. 3a, N1s peak deconvolution of an Aam plasma polymer film shows 2 peaks: a peak at 399.1 ± 0.2 eV which corresponds to C—$NH_{1,2}$ bonds, and a peak at 399.8 ± 0.1 eV which corresponds to CONH bonds. One should note that, N1s peak deconvolution was not possible for PPAac since the coating does not contain any nitrogen (Table 2).

High-resolution C1s and N1s spectra of PPAam/Aac and PPAac/Aam bipolar films present strong evidence for the presence of —NH_3^+ and —COO^- polar entities. In the case of the C1s peak, Fig. 2c shows the presence of a new peak at 288.7 eV for PPAam/Aac films compared to pure PPAam which reveals the formation of —COO^- groups. Also, as shown in Fig. 2d, comparing to the —COOH peak of the pure PPAac film at 289.2 eV, there is a lower binding energy of 288.7 eV (ΔeV = −0.5 eV) for the bipolar film; this shift is attributed to the formation of —COO^- groups.

The N1s spectra give additional proof of the formation of polar groups. As can be seen in Fig. 3b and c, a new peak at 401.4 ± 0.2 eV is present. This peak does not exist in pure PPAam film and is attributed to the formation of —NH_3^+ groups in the bipolar films. Beside the mentioned 288.7 eV C1s peak shift and the formed 401.4 eV N1s peak, all other peaks stayed at the same position.

Moreover, if we compare the COO^- and NH_3^+ peaks intensities for PPAam/Aac and PPAac/Aam films, we can see that the former films have a lot more polar groups. For the COO^- groups characterized by the peak at 288.7 eV in the C1s peak fitting, their percentage is much higher (16.7%; Fig. 2c) in the PPAam/Aac coating compared to the PPAac/Aam coating (1.7%; Fig. 2d). For the NH_3^+ groups characterized by the peak at 401.4 eV in the N1s peak fitting, their percentage is much higher (53.0%; Fig. 3b) in the PPAam/Aac coating compared to the PPAac/Aam coating (13.0%; Fig. 3c). This could be due to the proposed reaction mechanisms involved in the covalent bonding of the 2 layers forming the films depending on the sequence of deposition. Fig. 4 shows the proposed reaction mechanisms of bipolar films formed by (a) first depositing PPAam then PPAac and (b) first depositing PPAac then PPAam. Reaction preferences depends on the affinity each functional group has for the other which is limited by the bond dissociating energy of each functional site [17,18]. As can be seen, in the first reaction (a), one NH_2 group reacts with the double bonds of 2 Aac molecules, this yields a $N(R)_3$ with 2 COOH terminal groups which could subsequently react with 2 NH_2 groups to form polar NH_3^+/COO^- groups. In the second reaction (b), one COOH group reacts with one NH_2 group, this yields an amide group so no polar groups can be formed following this reaction. Different chemistries are therefore obtained depending on the deposition sequence.

3.1.2. WCA analysis

Fig. 5 shows the WCA values of pure PPAam, PPAac, PPAam/Aac and PPAac/Aam films. As can be seen, adding PPAac on top of PPAam in PPAam/Aac makes it considerably more hydrophilic (68.3° for PPAam and around 20° for the bipolar films). This is due to the increase in O% from 5.6% for PPAam to around 30% after Aac deposition (see Table 2). There was no noticeable change in WCA amongst the different PPAam/Aac films since as already mentioned an increase in O% for increased Aac deposition times is accompanied by a decrease in N%. On the other hand, adding PPAam on top of PPAac in PPAac/Aam makes it more hydrophobic (22.0° for PPAac and around 27° for the bipolar films). This is due to the considerable decrease in O% from 33.0% for PPAac to between 11.7 and 20.1% after Aam deposition (see Table 2). One should note that the WCA increase happened despite N incorporation; this is due to the fact that the percentage of nitrogen incorporated is lower than the percentage of O decrease going from PPAac to PPAac/Aam coatings, plus O is more electronegative than N which gives it a more pronounced effect on the surface wettability. For the different thicknesses of Aam deposits, it was observed that the WCA increases with Aam thickness increase. This is due to the decrease in O% going from a 40 nm to 80 nm Aam deposit.

3.2. Ageing study

Since the deposited coatings are intended to be used in biomedical applications which often require samples to be stored for a

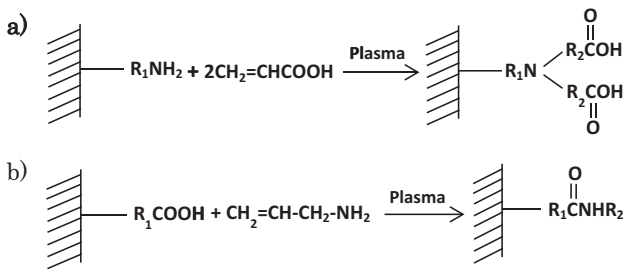

Fig. 4. Proposed reaction mechanisms of (a) PPAam/Aac and (b) PPAac/Aam bipolar films.

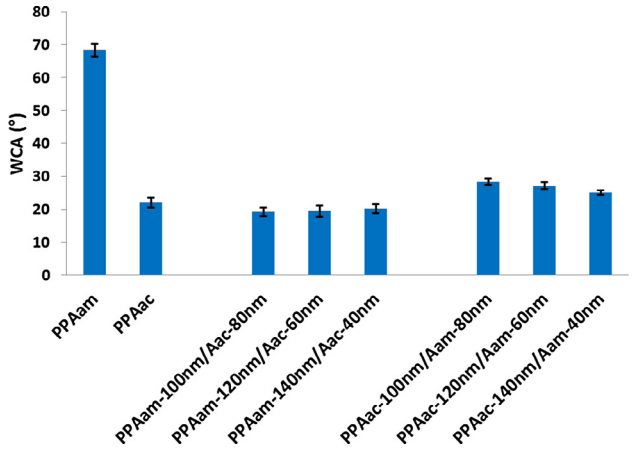

Fig. 5. WCA values of pure PPAam, PPAac, PPAam/Aac and PPAac/Aam films.

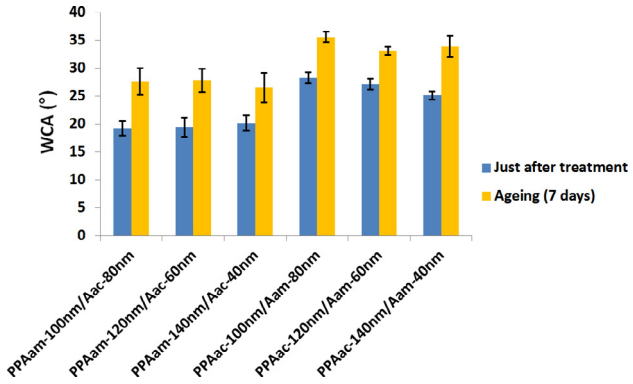

Fig. 6. WCA values (before and after ageing) of bipolar allylamine/acrylic acid films.

certain time period, evaluating film properties at the time of use is quite important. For that, bipolar films properties after storage in ambient atmosphere for 7 days were investigated using XPS and WCA analysis.

3.2.1. XPS

Table 3 shows the variations in nitrogen and oxygen percentages before and after ageing for the deposited bipolar films. For nitrogen variation, as can be seen, for both bipolar series, the nitrogen percentage decreased with a slightly higher reduction for the PPAac/Aam coatings. For oxygen variation, as can be seen, for PPAam/Aac coatings, the oxygen percentage decreased after ageing. However, for PPAac/Aam coatings, the oxygen percentage increased after ageing. Moreover, there was no significant difference in Δ[N]% and Δ[O]% amongst the different films in each bipolar series.

Nitrogen reduction in both bipolar series and oxygen reduction in PPAam/Aac coatings after ageing is associated to the fact that, in time, polar structures migrate away from the surface in order to minimize its free energy [19]. On the other hand, oxygen increase in PPAac/Aam coatings after ageing is attributed to amine oxidation.

3.2.2. WCA

Fig. 6 shows the variations in WCA values before and after ageing for the deposited bipolar films. As can be seen, for both bipolar series, WCA increases after ageing; this can be correlated to the XPS results where polar groups were seen to mostly move away from the surface. Despite the observed oxygen increase in PPAac/Aam coatings, its wettability is decreasing which can be due to the fact that XPS is a 10 nm in depth surface characterization technique whereas WCA is a top layer surface characterization technique. Overall ageing wettability behavior of the films of each bipolar series did not seem to depend on the thickness of the second deposited polymer coating.

3.3. Stability test

Since the deposited coatings are intended to be used in biomedical applications, coating stability in aqueous environment is quite important. For that, bipolar films properties after soaking in D.I. water for 7 days were investigated using XPS and OPS analysis.

3.3.1. XPS

Table 4 shows the variations in nitrogen and oxygen percentages before and after soaking for the deposited bipolar films. For nitrogen variation, as can be seen, for PPAam/Aac coatings, nitrogen percentage does not vary much after soaking. This is probably due to the fact that nitrogen is mostly incorporated in these films as NH_3^+ groups which are quite stable due to COO^- interactions. This is not the case for PPAac/Aam coatings where the% of NH_3^+ formed is much lower (Fig. 3c) and therefore nitrogen functionalities are less stabilized which leads to their dissolution and thus to a decrease in nitrogen percentage after soaking. It can also be observed that the thinner the Aam coating is, the lower the N% is after soaking. This is probably due to the fact that dissolution will have a bigger impact in this case since the closer to the 1st layer (Aac) we get the more rearrangements there will be and the lower the N% will be.

Table 3
Nitrogen and oxygen percentages (before and after ageing) of bipolar allylamine/acrylic acid films.

Sample	Just after treatment	Ageing (7 days)	Δ[N] (%)
	[N] (%)		
PPAam-100 nm/Aac-80 nm	3.1 ± 0.6	2.1 ± 0.6	1.0 ± 0.0
PPAam-120 nm/Aac-60 nm	4.3 ± 0.9	3.4 ± 0.6	0.9 ± 0.3
PPAam140 nm/Aac40 nm	6.0 ± 0.5	4.9 ± 0.6	1.1 ± 0.1
PPAac-100 nm/Aam-80 nm	13.5 ± 0.2	11.2 ± 0.6	2.3 ± 0.4
PPAac-120 nm/Aam-60 nm	13.0 ± 0.3	10.7 ± 0.7	2.3 ± 0.4
PPAac-140 nm/Aam-40 nm	9.9 ± 0.5	7.9 ± 1.0	2.0 ± 0.5
	[O] (%)		Δ[O] (%)
PPAam-100 nm/Aac-80 nm	32.0 ± 0.8	24.7 ± 0.9	7.3 ± 0.1
PPAam-120 nm/Aac-60 nm	29.2 ± 1.5	24.0 ± 0.8	5.2 ± 0.7
PPAam140 nm/Aac40 nm	29.5 ± 1.1	22.9 ± 0.4	6.6 ± 0.7
PPAac-100 nm/Aam-80 nm	11.7 ± 1.0	13.7 ± 1.1	2.0 ± 0.1
PPAac-120 nm/Aam-60 nm	14.2 ± 1.1	16.7 ± 0.6	2.5 ± 0.5
PPAac-140 nm/Aam-40 nm	20.1 ± 1.6	23.0 ± 1.2	2.9 ± 0.4

Table 4
Nitrogen and oxygen percentages (before and after stability) of bipolar allylamine/acrylic acid films.

Sample	Just after treatment	Stability (7 days)
	[N] (%)	
PPAam-100 nm/Aac-80 nm	3.1 ± 0.6	3.0 ± 0.6
PPAam-120 nm/Aac-60 nm	4.3 ± 0.9	4.1 ± 0.6
PPAam140 nm/Aac40 nm	6.0 ± 0.5	6.0 ± 0.6
PPAac-100 nm/Aam-80 nm	13.5 ± 0.2	6.4 ± 0.6
PPAac-120 nm/Aam-60 nm	13.0 ± 0.3	4.3 ± 0.2
PPAac-140 nm/Aam-40 nm	9.9 ± 0.5	3.4 ± 0.3
	[O] (%)	
PPAam-100 nm/Aac-80 nm	32.0 ± 0.8	26.9 ± 0.7
PPAam-120 nm/Aac-60 nm	29.2 ± 1.5	25.0 ± 1.0
PPAam140 nm/Aac40 nm	29.5 ± 1.1	21.3 ± 1.1
PPAac-100 nm/Aam-80 nm	11.7 ± 1.0	23.1 ± 1.5
PPAac-120 nm/Aam-60 nm	14.2 ± 1.1	24.8 ± 1.3
PPAac-140 nm/Aam-40 nm	20.1 ± 1.6	26.8 ± 1.2

For oxygen variation, as can be seen, for PPAam/Aac coatings, oxygen percentage decreases after soaking which is due to the dissolution of some oxygen functionalities. Moreover, as was the case for nitrogen reduction in PPAac/Aam coatings, the thinner the Aac coating the lower the O% is after soaking. However, for PPAac/Aam coatings, O% increased after soaking. This can be attributed to the lower percentage of polar groups formed during PPAac/Aam deposition: the lower amount of ionic bonds formed between the layers yields a lower stability of the films. So it can already be speculated that a considerable thickness of the Aam layer has been dissolved in the water thus leading to an increase in surface oxygen percentage (this can be confirmed with the upcoming OPS results). The thinner the original Aam layer, the closer we get to the Aac coating and the higher the O% obtained after soaking.

Amongst the prepared PPAam/Aac films, the most stable films which maintained the highest O% after soaking are PPAam-100 nm/Aac-80 nm and PPAam-120 nm/Aac-60 nm. And amongst the prepared PPAac/Aam films, the most stable film which maintained the highest N% after soaking is PPAac-100 nm/Aam-80 nm.

3.3.2. OPS

Fig. 7 shows the change in thickness for the prepared bipolar films before and after soaking in deionized water for 7 days. As seen from this Figure, PPAam/Aac films are more stable in water than PPAac/Aam films which is consistent with the previously shown XPS results and is believed to be due to the higher amount of ionic bonds in PPAam/Aac films leading to a higher stability of the coating. Amongst the various single-layers thickness of each bipolar films series, no particular difference in coatings stability was depicted.

As can also be noticed, large standard deviations were obtained. This is probably due to a non-homogeneous surface dissolution which is not occurring in a layer by layer mode but in a more localized way thus creating holes in the surface. This can be attributed to the bipolar nature of the coatings where film removal is harder when bipolar interactions are present (NH_3^+/COO^-) and easier when bipolar interactions are absent (neutral N and O functionalities).

3.4. Cell tests

For biocompatibility evaluation, cell tests were performed for untreated, PPAam, PPAac, and two selected bipolar films with different deposition sequence. Cell viability percentage after 1 and 7 days culture are shown in Fig. 8. As can be seen, PPAac coatings showed low cell affinity and extensive standard deviations compared to the other plasma treated samples. This is attributed to the relatively limited stability of the coating and the substantial hole-forming dissolution of the film where cells grow preferentially. This was confirmed by OPS measurements performed before and after soaking (results not shown here) where film loss and standard deviations were considerably high. As can also be seen, all other treated films showed better cell viability than the untreated UHMWPE. After 1 day culture, cell viability was higher for both bipolar films compared to the PPAam film with a higher cell viability percentage for the PPAam/Aac film. And after 7 days, cell viability remained higher on the PPAam/Aac film compared to both PPAam and PPAac/Aam films that showed close cell viability percentages when taking their standard deviations into account.

This suggests that the NH_3^+/COO^- bipolar groups act as reactive binding sites within the network. This leads to a higher cell density after 1 day culture on the bipolar coatings as compared to the PPAam coating with a higher cell density on the PPAam/Aac ionic binding sites loaded film. The higher cell density obtained after 7 days culture on the PPAam/Aac film can be linked to the greater film stability which is correlated to the considerable amount of polar groups incorporated during plasma treatment.

For the bipolar coatings, a reduction in cell viability after 7 days culture as compared to 1 day culture was also observed; this can be linked to the stability behavior of the films. As is evident, the reduction is very minor in the case of PPAam/Aac coating which showed greater stability and is more noticeable in the case of PPAac/Aam coating which showed lower stability.

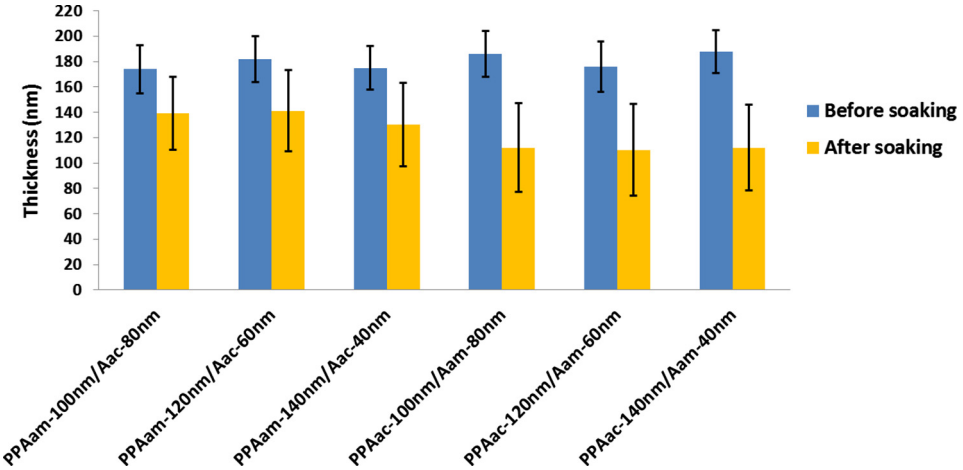

Fig. 7. Thicknesses of bipolar allylamine/acrylic acid films before and after immersion in deionized water for 7 days.

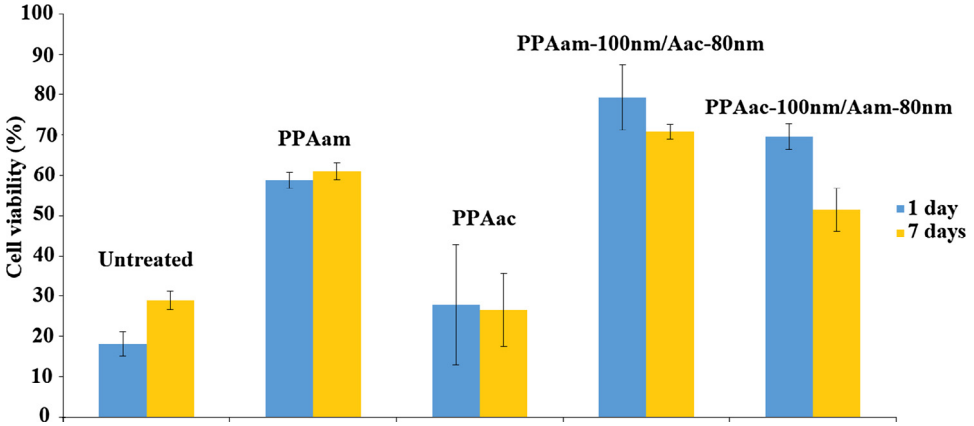

Fig. 8. Cell viability percentage after 1 and 7 days cell proliferation test for untreated, PPAam, PPAac, PPAam/Aac and PPAac/Aam UHMWPE samples.

4. Conclusion

In this study, allylamine and acrylic acid bipolar coatings were deposited onto UHMWPE using a dielectric barrier discharge. Various films were prepared by changing the single-layer thickness of both PPAam and PPAac and two film series were obtained by changing the deposition sequence of both layers. Chemical and physical properties of these coatings were investigated and their ageing and stability behaviors after storage at ambient atmosphere and soaking in D.I. water for a period of 7 days, respectively, were evaluated. Results showed that, after plasma deposition, bipolar NH_3^+/COO^- groups were present in both prepared film series with a higher amount present in the PPAam/Aac films. For the ageing test, results showed that both bipolar series underwent surface modification after storage which was shown via XPS and WCA analysis and this change depended on the deposition sequence and not on the thickness of the deposited layers. For the stability test, XPS and OPS results showed that PPAam/Aac films were more stable than PPAac/Aam films which is due to the higher amount of bipolar groups formed in the former films. Stability behavior depended on both the deposition sequence and the thickness of the deposited layers with the highest surface chemistry stability obtained for PPAam-100 nm/Aac-80 nm, PPAam-120 nm/Aac-60 nm, and PPAac-100 nm/Aam-80 nm coatings. Moreover, cell tests were performed in order to evaluate the cell-material interaction properties of these films. Results showed that, after 1 day cell culture, cell viability was higher on the bipolar films as compared to PPAam and PPAac with a higher cell density obtained for the PPAam/Aac film; this was attributed to the presence of bipolar groups that act as biomolecule binding sites. And after 7 days culture, cell density was seen to decrease as compared to after 1 day culture which was attributed to the stability behavior of the coatings but remained the highest on the PPAam/Aac film which was attributed to its higher stability.

Acknowledgments

This research was supported by a grant (G.0516.13N) from the *Research Foundation Flanders* (FWO) and has also received funding from the European Research Council (ERC) under the European Union's Seventh Framework Program (FP/2007-2013)/ERC Grant Agreement no. 279022 (PLASMAPOR).

References

[1] D.E. Robinson et al., Surface gradient of functional heparin, Adv. Mater. 20 (6) (2008) 1166–1169.
[2] J. Xu, K.K. Gleason, Conformal, amine-functionalized thin films by initiated chemical vapor deposition (iCVD) for hydrolytically stable microfluidic devices, Chem. Mater. 22 (5) (2010) 1732–1738.
[3] L. Detomaso et al., Stable plasma-deposited acrylic acid surfaces for cell culture applications, Biomaterials 26 (18) (2005) 3831–3841.
[4] J. Charnley, Surgery of the hip-joint, British Med. J. 1 (5176) (1960) 821.
[5] B. Cales, Zirconia as a sliding material: histologic, laboratory, and clinical data, Clin. Orthopaed. Relat. Res. 379 (2000) 94–112.
[6] K.S. Katti, Biomaterials in total joint replacement, Colloids Surf. B 39 (3) (2004) 133–142.
[7] G. Willmann, Ceramics for total hip replacement-what a surgeon should know, Orthopedics 21 (2) (1998) 173–177.
[8] G. Lewis, Polyethylene wear in total hip and knee arthroplasties, J. Biomed. Mater. Res. 38 (1) (1997) 55–75.
[9] M. Heuberger et al., Protein-mediated boundary lubrication in arthroplasty, Biomaterials 26 (10) (2005) 1165–1173.
[10] M.R. Widmer et al., Influence of polymer surface chemistry on frictional properties under protein-lubrication conditions: implications for hip-implant design, Tribol. Lett. 10 (1–2) (2001) 111–116.
[11] W. Norde, C.E. Giacomelli, BSA structural changes during homomolecular exchange between the adsorbed and the dissolved states, J. Biotechnol. 79 (3) (2000) 259–268.
[12] P. Ying et al., Competitive protein adsorption studied with atomic force microscopy and imaging ellipsometry, Colloids Surf. B 32 (1) (2003) 1–10.
[13] P. Cools et al., A stability study of plasma polymerized acrylic acid films, Appl. Surf. Sci. (2017).
[14] G. Aziz et al., Plasma parameters effects on the properties, aging and stability behaviors of allylamine plasma coated ultra-high molecular weight polyethylene (UHMWPE) films, Appl. Surf. Sci. 409 (2017) 381–395.
[15] X. Wang et al., Structural characterization and mechanical properties of functionalized pulsed-plasma polymerized allylamine film, Surf. Coat. Technol. 204 (18) (2010) 3047–3052.
[16] R. Jafari et al., Stable plasma polymerized acrylic acid coating deposited on polyethylene (PE) films in a low frequency discharge (70 kHz), Reactive Funct. Polym. 66 (12) (2006) 1757–1765.
[17] O.S. Kolluri, R.G. Johanson, Plasma Deposited Substrate Structure, Google Patents, 1999.
[18] L. Denis et al., Deposition of functional organic thin films by pulsed plasma polymerization: a joint theoretical and experimental study, Plasma Processes Polym. 7 (2) (2010) 172–181.
[19] T.R. Gengenbach, H.J. Griesser, Compositional changes in plasma-deposited fluorocarbon films during ageing, Surf. interface analysis 26 (7) (1998) 498–511.